Available online at www.sciencedirect.com
SCIENCE DIRECT®
Journal of Photochemistry and Photobiology A: Chemistry 170 (2005) 113–121
Journal of Photochemistry and Photobiology A:Chemistry
www.elsevier.com/locate/jphotochem

Complexation studies of chlorophyll a with trinitro substituted fluorene derivates

R. Smalley, M. O'Brien, S. Raber, A. Amonge, J. Pedigo, T. Buthelezi*

Department of Chemistry, Western Kentucky University, Bowling Green, KY 42101, USA

Received 1 June 2004; received in revised form 30 July 2004; accepted 4 August 2004

Abstract

Ground and excited state complexes of chlorophyll a from spinach with fluorene and trinitro substituted fluorene derivatives have been studied via absorption and fluorescence spectroscopy. Solvent effects on the binding of chl a to these fluorene molecules have been monitored in acetonitrile and dichloromethane at ambient temperature. The association constants (K_a) and the Stern-Volmer constants (K_{sv}) of the investigated complexes were larger in acetonitrile. Molecular modeling results of these systems suggest that the total binding energy of chl a/acceptor complex is dependent on the long-range (dispersion and electrostatic) interactions. Free energies of chl a/acceptor systems scale with the acceptor's dipole moment, electron affinity and dispersion interactions.

Keywords: Fluorescence quenching; Donor–acceptor; Dipole–dipole interactions; Molecular modeling; Solvent effects; Association constant

1. Introduction

Absorption of light from the sun by chlorophyll molecules increases the population of excited electronic states. Excited chlorophyll pigments induce intermolecular electron transfer interactions in photosynthetic systems. In green plants, the excited chromophore (chlorophyll a) serves as an electron donor, and eventual electron acceptor is typically a quinone molecule. Electron transfer interactions between chlorophyll and acceptor molecules such as quinones [1–5] and nitro aromatic compounds [6–9] have been studied extensively in order to understand the mechanisms involved in photosynthesis. However, the mechanisms involved in excitation energy and electron transfers in photosystems I and II (PSI and PSII, respectively) are not yet fully understood [10]. Recently, X-ray crystal structures of PSI [11] and PSII [12] have been reported. Breakthroughs have been made towards the understanding of PSI, whereas a refined crystal structure of ~3 Å resolution or better has not yet been obtained for PSII. It is anticipated that when the latter is acquired, our results in this study will contribute towards the understanding of the electron transfer mechanism involved in PSII.

Fluorescence emission is one of the several competing de-excitation pathways of the excited chlorophyll molecules. Other mechanisms for the excited chlorophyll molecules to return to the ground state include phosphorescence, photochemistry and heat dissipation. Fluorescence quenching of chlorophyll can be used to study aspects of photosynthesis since the fluorescence yield is the lowest when phosphorescence, photochemistry and heat dissipation are the highest. Previous studies have shown that chlorophyll a (chl a) forms 1:1 complexes with the following nitro aromatic acceptors; 2-(2,4,7-trinitro-fluoren-9-ylidene)-malononitrile (TNFM) [6], 2,4,7-trinitrofluorenone (TNFO) [7] and *sym*-trinitrobenzene (TNB) [9]. Studies indicate that the site of interaction of TNB with chl a is confined to the α and β positions (ring II) of the macrocycle, and the electron rich cyclopentanone (ring V) does not take part in π-donation. It is also suggested that other trinitro acceptors will bind in the same position [7]. We have conducted molecular mechanics calculations in this study to provide theoretical support for the proposed binding site. The

* Corresponding author. Tel.: +1 270 745 6998; fax: +1 270 745 5361.
E-mail address: thandi.buthelezi@wku.edu (T. Buthelezi).

1010-6030/$ – see front matter © 2004 Elsevier B.V. All rights reserved.
doi:10.1016/j.jphotochem.2004.08.005

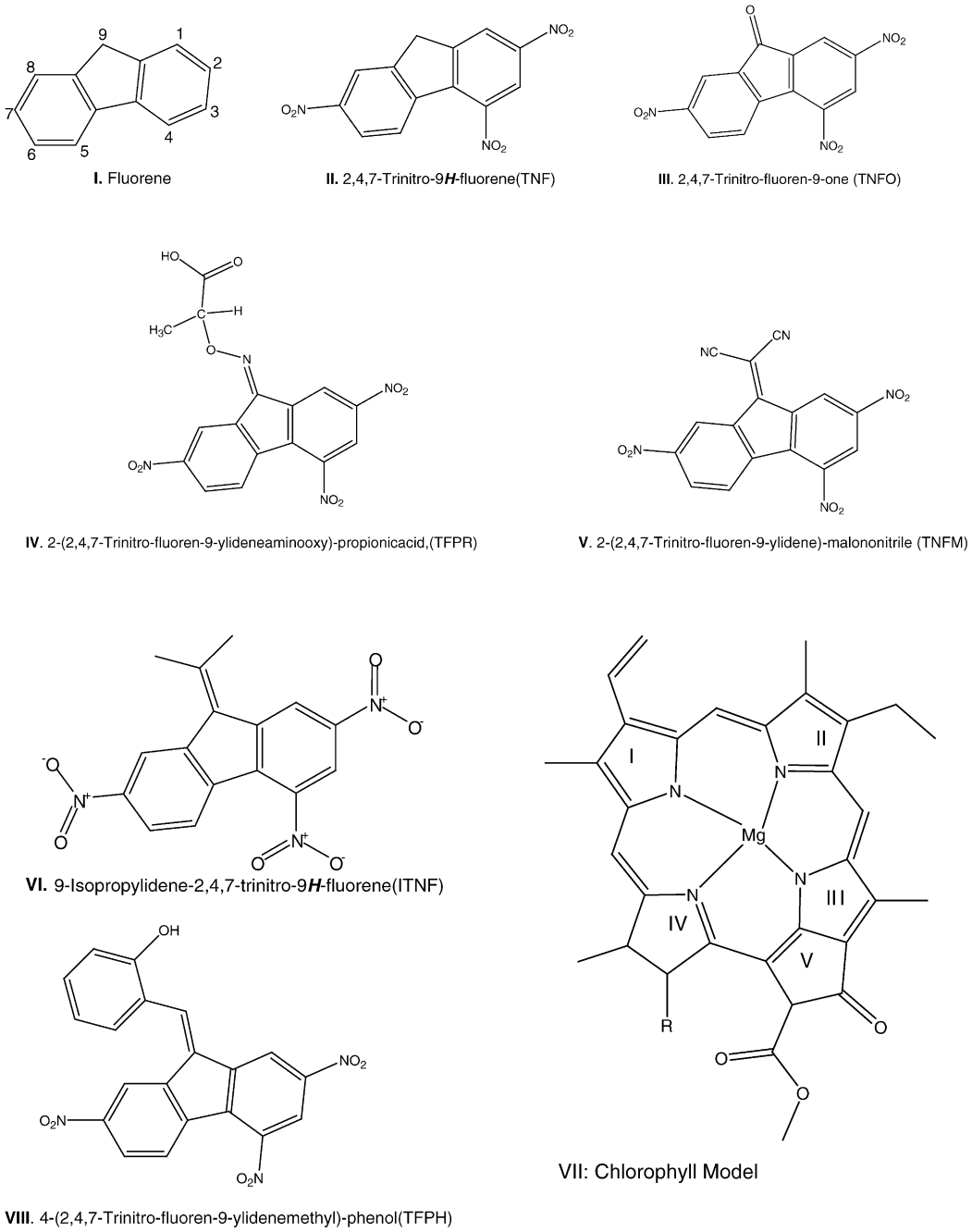

Fig. 1. Fluorene derivatives and the model structure of chl a (I–VIII) used in the Gaussian 03 DFT and PC Model 7.5 calculations. Hydrogen atoms are not shown for simplicity.

model structure of chl a [13] and the acceptor molecules investigated in this study are shown in Fig. 1. Previous studies indicate that the phytyl group has no effect on the excited state properties of chl a [14]. Hence, in the chlorophyll model, a hydrogen atom replaces the phytyl group, represented by R. The latter also facilitates in reducing computational cost.

In vitro, very little is known about the geometry of the chl a/acceptor complex at the binding site. We report in this paper seven optimized structures of the complexes of chl a with fluorene and its derivatives. Chlorophyll –complexes (π–π interaction) were studied with PC Model 7.5 software package [15] using the molecular mechanincs (MMX) force field and these results are presented in Table 1. The van der Waals (VDW) interactions between the donor (chl a) and acceptor (fluorene derivatives) were calculated. The enthalpy of the complex (ΔH_{calc}) was determined from the standard expression: $\Delta H^{\text{o}}_{\text{calc}} = H^{\text{o}}_{\text{f}}\,(\text{complex}) - [H^{\text{o}}_{\text{j}}\,(\text{donor}) + H^{\text{o}}_{\text{j}}\,(\text{acceptor})]$, where H^{o}_{f} is the standard heat of formation. Moreover, we have used Gaussian W03 [16] to opti-

Table 1
Calculated interaction energies between chl a and acceptor molecules (π–π configuration) in the gas phase at 300 K, using PC Model 7.5 software package with MMX force field

Donor–acceptor complex	$-\Delta H_{calc}$ (kcal/mole)	VDW (kcal/mole)	Distance (Å) Mg–C_9[a]
chl a–fluorene	14.2	−12.8	3.39
chl a–TNFO	66.6	1.98	4.02
chl a–TNF	62.4 (19.4)[b]	0.790	4.45
chl a–TFPH	49.5	6.12	4.42
chl a–TFPR	60.4	0.470	4.17
chl a–ITNF	50.8	2.82	4.36
chl a–TNFM	59.4 (5.02)[b]	4.73	4.11

[a] Distance between Mg and 9-carbon atom.
[b] Ref. [17].

mize the monomer structures (donor and acceptors) at the density functional theory (DFT) level with the Becke-style 3-Parameter, Lee-Yang-Parr (B3LYP) correlation functional with 3-21G basis set; dipole moments and electron affinities of the minimized structures are presented in Table 2. The 3-21G basis set was chosen to minimize computational cost. Structures of molecules used for theoretical investigations are presented in Fig. 1.

In these chl a/acceptor systems the important long-range forces are dipole–dipole and dispersion forces. Various functional groups were substituted at position 9 of the trinitro-fluorene molecules. The acceptor strength of aromatic compounds is enhanced by substitution of strong electron withdrawing functional groups. In this paper we also present spectroscopic results of absorption and fluorescence quenching studies of chl a with fluorene and three new trinintro derivatives of fluorene: 2-(2,4,7-trinitro-fluoren-9-ylideneaminooxy)-propionic acid (TFPR); (2,4,7-trinitro-fluoren-9-ylidenemethyl)-phenol (TFPH); and 9-isopropylidene-2,4,7-trinitro-9H-fluorene (ITNF). Solvent effects were also investigated by studying these systems in acetonitrile and dichloromethane at room temperature. Theoretical models (DFT and MMX) are used to support experimental data.

Table 2
Calculated electron affinities (EA), and dipole moments of acceptor (or quencher) molecules using Gaussian W03 with B3LYP functional and 3-21G basis set

Molecule	$EA_{calculated}$ (eV)	$EA_{experimental}$ (eV)	Dipole moment (D)
chl a	–	–	4.86, 4.33[a]
Fluorene	−0.84 (−0.68)[b]	0.700[c]	0.52, 0.82[d]
TNF	2.37 (2.42)	–	2.61
ITNF	2.36 (2.40)	–	4.48
TFPR	2.51 (2.56)	–	2.56
TFPH	2.30 (2.36)	–	7.06
TNFO	2.78 (2.8)	2.05[e]	0.982
TNFM	3.21 (3.25)	2.45[e]	2.54

[a] Dipole moment computed using PC Model 7.5 software package [15] with MMX force field.
[b] Electron affinities in parenthesis are zero-point energy corrected with the usual scale factor of 0.9804 [20].
[c] Ref. [21].
[d] Ref. [20].
[e] Ref. [22].

2. Experimental procedures

The following chemicals were purchased from Aldrich: Chlorophyll a from spinach, fluorene, TFPR, TFPH, ITNF, spectrophotometric grade solvents (CH_3CN and CH_2Cl_2), and were used as received. A stock solution of chl a was prepared by dissolving 1 mg of chl a, into a 10 mL volumetric flask and filled to the mark with either CH_3CN or CH_2Cl_2. The absorbance of the prepared stock solution was measured using a Shimadzu model UV-2101 PC (UV–vis) spectrophotometer. Beer's law was used to calculate the concentration of the chl a stock solution ($\varepsilon_{CH_3CN} = 7 \times 10^4$ and $\varepsilon_{CH_2Cl_2} = 6.1 \times 10^4\ M^{-1}\ cm^{-1}$ [17]). The ratio of the intensities of the Soret band and the Q_{0-0} band was 1.31, in agreement with previously reported value [17,18]. Dilutions were made to this stock solution until a concentration of 1×10^{-5} M was obtained. This concentration is low enough to ensure that chl a exists in the monomeric state. For each absorption experiment, the concentration of chl a was kept constant. A volume of 3.4 mL of the 1×10^{-5} M chl a (donor molecule) solution was measured into a quartz cuvette. The acceptor molecule (TFPR, TFPH, ITNF or fluorene) was introduced to this volume, with constant stirring, in 1 mg increments up to 6 mg. The absorption spectrum was collected a few minutes following each addition.

For fluorescence measurements, a stock solution of 3×10^{-6} M chl a in a chosen solvent was prepared. The concentration was confirmed by measuring the absorbance spectrum. A stock solution of the acceptor molecule was also prepared at a concentration of 2×10^{-3} M. From this concentration, diluted solutions of the acceptor molecule at varying concentrations were prepared. These solutions were then complexed (1:1, by volume) with a constant concentration, 3×10^{-6} M, of chl a solution, and the fluorescence spectra of the unbound chl a solution and its donor–acceptor complex were acquired. In all fluorescence samples the final concentration of chl a in solution was kept constant at 1.5×10^{-6} M. The variation of the chl a's fluorescence intensities was monitored as a function of the quencher's concentration in a given environment at constant temperature, 25 °C. All solutions were equilibrated in a water bath at 25 °C. Laser induced fluorescence, LIF, was used for the acquisition of the fluorescence data. A nitrogen-pumped dye laser system was used for excitation. The wavelengths of the isosbestic points (when present) were used for excitation, alternatively, wavelength regions that showed minimum variations in absorbance values as a function of quencher concentration were selected. An Andor ICCD camera coupled to Oriel MS260i spectrograph was used for data collection. A filter was placed prior to the entrance slit of the spectrograph to block the excitation wavelength. The fluorene and its derivatives employed do not absorb or fluoresce

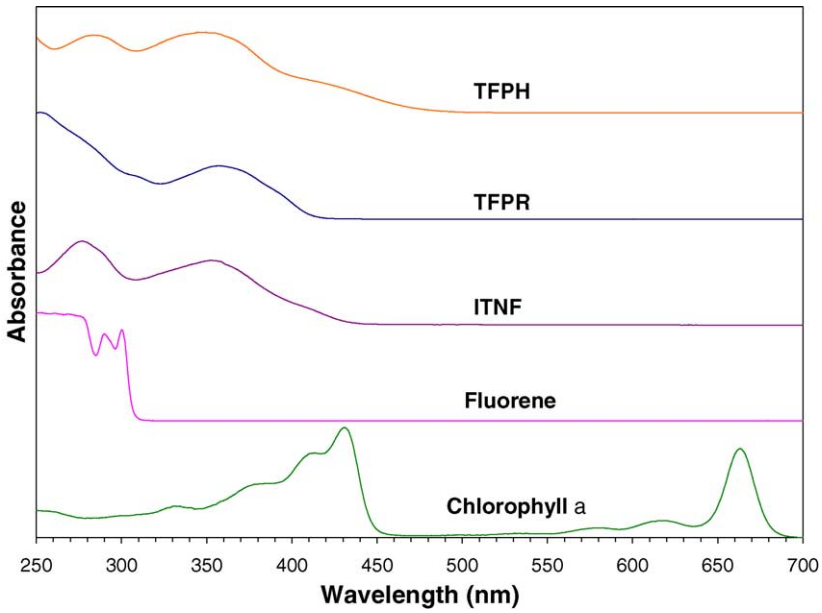

Fig. 2. UV–vis absorption spectra of chlorophyll a from spinach, fluorene, 9-isopropylidene-2,4,7-trinitro-9H-fluorene (ITNF), 2-(2,4,7-trinitro-fluoren-9-ylideneaminooxy)-propionic acid (TFPR), and 2-(2,4,7-trinitro-fluoren-9-ylidenemethyl)-phenol (TFPH) in dichloromethane.

at the wavelength of excitation and emission of chl a as shown in Fig. 2.

3. Results and discussion

3.1. Ground state characteristics

Table 3 summarizes ground state parameters of chl a interactions with various electron acceptors in dichloromethane and acetonitrile. Absorption maxima ($\lambda_{abs\ max}$), association constants (K_a) and free energies (ΔG) of the investigated systems are presented. Changes in the absorbance spectrum of chl a upon addition of acceptor molecule were monitored as shown in Figs. 3 and 4. Isosbestic points were not observed for the interactions of chl a with fluorene, however, they were detected at 450 and 560 nm for chl a/TFPR (Fig. 4) and only at 595 nm for chl a/TFPH (figure not shown) systems in dichloromethane. However, the chl a/TFPR system undergoes loss of Mg metal since chlorophyll readily demetalates in an acid. Appearance of new peaks at 606, 536 and 505 nm confirms that demetalation has occurred. Pheophytin (Mg free chlorophyll) in dichloromethane absorbs at 612, 538 and 507 nm, the shifts are due to the presence of TFPR acceptor. Formation of an isosbestic point further supports 1:1 complexation. Absorption data were not acquired for ITNF because the vendor discontinued the product. The absorption data were fitted to a Nash plot [19]; linearity of these plots confirmed that a 1:1 complex was formed between chl a and the acceptor molecule as shown in Fig. 5. The K_a values were determined from the *y*-intercept of these plots. In all investigated systems (except chl a/TFPH), the ground state K_a of the chl a to the acceptor are larger in a more polar solvent, acetonitrile. This indicates greater stabilization of the charge transfer interaction in acetonitrile. Our results are in agreement with most systems reported in literature [1,6].

In the absence of specific solute–solvent interactions, such as hydrogen bonding, the changes in fluorescence energy with solvent can often be related to the dielectric constant of the solvent. These energy changes are termed "polarization shifts" and are credited to polarization of solvent molecules induced by the transition dipole of the solute. Polarization shifts involve a shift of energy of the fluorescence maximum energy as a function of the solvent polarity. Permanent dipole–dipole forces may also be of importance. Previous

Table 3
Ground state binding constants K_a, absorption maximum, $\lambda_{abs\ max}$, and Gibb's energy of chl a with various acceptor molecules in CH_3CN and CH_2Cl_2 at 25 °C

System	Solvent	$\lambda_{abs\ max}$ (nm)	K_a (M^{-1})	$-\Delta G$ (kcal/mol)
chl a only	CH_3CN	660	–	–
	CH_2Cl_2	663	–	–
chl a–fluorene	CH_3CN	660	60	2.41
	CH_2Cl_2	663	20	1.77
chl a–TFPR	CH_3CN	661	2370	4.59
	CH_2Cl_2	663	450	3.61
chl a–TFPH	CH_3CN	661	300	3.37
	CH_2Cl_2	662	3220	4.78
chl a–TNF[a]	CH_2Cl_2	662	90	2.68
chl a–TNFM[b]	CH_3CN	660	3240	4.78
	CH_2Cl_2	660	2200	4.57
chl a–TNFO[c]	CH_2Cl_2	662	103	2.75

Association constants and free energies are not applicable for chl a only system.
[a] Ref. [17].
[b] Ref. [6].
[c] Ref. [7].

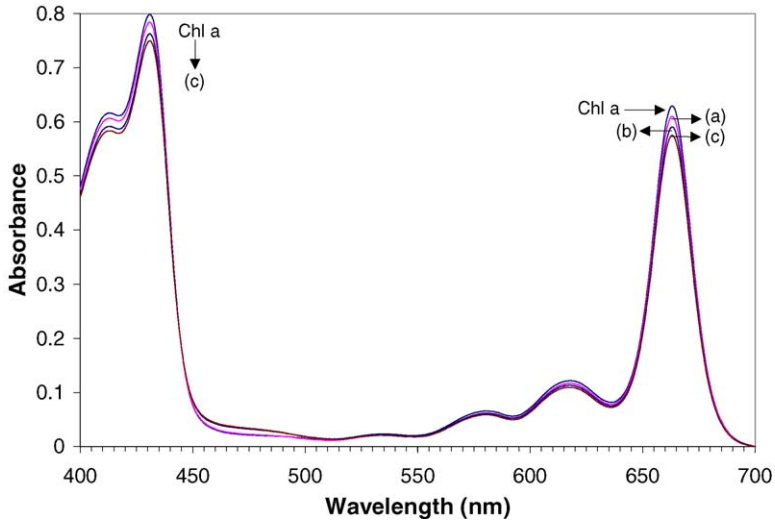

Fig. 3. Changes in the absorption spectrum of chl a in dichloromethane, upon addition of fluorene: (a) 3.5×10^{-3} M, (b) 7.1×10^{-3} M and (c) 1.1×10^{-2} M.

studies [6,7] have observed electrostatic effects upon fluorescence energies. These studies indicate that many organic molecules become considerably more polar when electronically excited. In this study we observed different trends in measured excited state properties versus ground state parameters, indicative of different geometries in these electronic states.

3.2. Excited state characteristics

A quantum of radiation is emitted in fluorescence that will be of lower energy on average than the quantum absorbed by the molecule. This change in photon energy results in a shift of the fluorescence spectrum to longer wavelengths, relative to the absorption spectrum. This is known as a Stokes Shift ($\Delta\nu$). The Stokes Shift energy represents the magnitude of vibrational relaxation in each system. These values are tabulated in Table 4, along with the emission maxima (λ_{emmax}) and the half-quenching concentrations ($Q_{1/2}$) of the complexes in solution. The $Q_{1/2}$ value represents the amount of quencher necessary to reduce the initial intensity of the chl a fluorescence by a factor of one half. Hence, the smaller the $Q_{1/2}$ value, the more effective the quencher molecule. No emission maximum was reported for the TNF system [17], and both TNF and TNFO were only investigated in CH_2Cl_2. Absorption data were not acquired for the ITNF system in this study, thus no Stokes Shift value is reported for this complex.

Fig. 6 shows an inverse relationship between the fluorescence intensity and the concentration of the acceptor

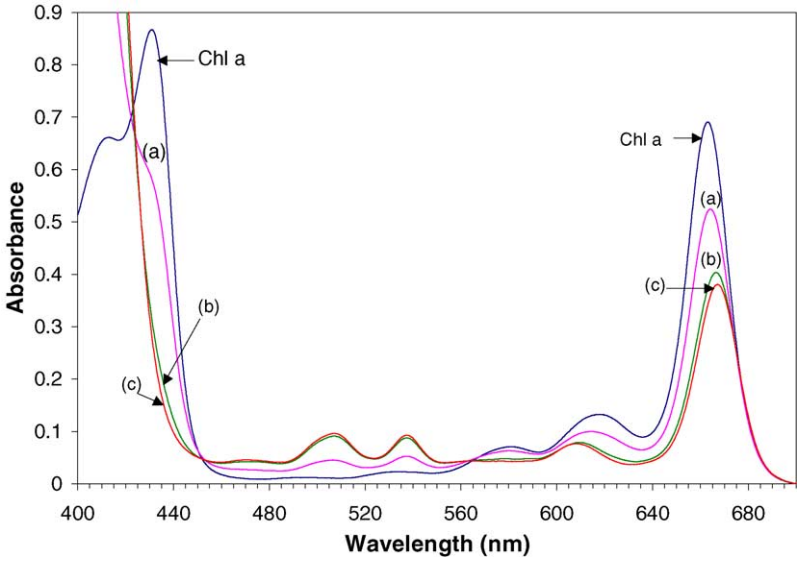

Fig. 4. Demetalation of chl a in dichloromethane, upon addition of TFPR: (a) 7.3×10^{-4} M, (b) 1.4×10^{-3} M and (c) 2.2×10^{-3} M. Isosbestic points were observed at 451 and 563 nm.

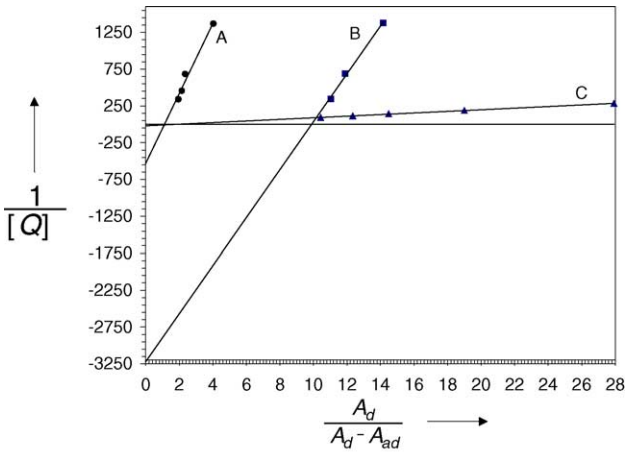

Fig. 5. Nash plots for the interactions of chl a with: (A) TFPR (●), (B) TFPH (■) and (C) fluorene (▲) in dichloromethane at 25 °C.

(ITNF). The intensities decreased as the concentration of the acceptor molecule increased. A linear Stern-Volmer plot is shown in Fig. 7, and the Stern-Volmer constant (K_{SV}) is determined from the slope of this line. The measured K_{SV} values for all the investigated systems are presented in Table 4.

3.3. Molecular modeling

Minimized energies of all the anion counterpart of the quenchers in Fig. 1 were also computed. The zero point energy (ZPE) corrected energy differences, $\Delta E_{zpe\_corrected}$, in pairs of molecules [$\Delta E_{zpe\_corrected} = E_{neutral} - E_{anion}$] were computed and are listed as the calculated electron affinities.

Table 4
Excited state complexation parameters: emission maximum, $\lambda_{em\ max}$, Stokes Shift, Stern-Volmer constants, K_{sv} of chl a with various acceptor molecules in CH_3CN and CH_2Cl_2 at 25 °C

System	Solvent	$\lambda_{em\ max}$ (nm)	Stokes Shift $\Delta\nu$ (cm^{-1})	K_{sv}	$Q_{1/2}$ (mM)
chl a only	CH_3CN	670	226.1	–	–
	CH_2Cl_2	672	202.0	–	–
chl a–fluorene	CH_3CN	670	226.1	40	25.0
	CH_2Cl_2	673	224.1	70	14.0
chl a–TFPR	CH_3CN	669	180.9	2070	4.80
	CH_2Cl_2	672	224.8	160	6.25
chl a–ITNF	CH_3CN	670	–	480	2.10
	CH_2Cl_2	670	–	220	4.50
chl a–TNF[a]	CH_2Cl_2	–	–	260	3.85
chl a–TNFM[b]	CH_3CN	669	203.8	3230	0.310
	CH_2Cl_2	670	226.1	1850	0.540
chl a–TNFO[c]	CH_2Cl_2	669	158.1	260	3.85

Association constants and free energies are not applicable for chl a only system; Stokes Shifts were not determined for ITNF and TNF systems.
[a] Ref. [17].
[b] Ref. [6].
[c] Ref. [7].

The global minima of optimized structures were located by: (1) utilizing the Guassian convergence criteria and (2) verifying that there were zero imaginary vibrational frequencies. Zero point energy electron affinities were corrected with the usual scale factor of 0.9804 [20]. The trends of calculated electron affinities follow the one observed in experimental values [21,22] as shown in Table 3. Moreover, our computed electron affinity values of fluorene, −0.84(−0.68) eV at B3LYP/3-21G, are in excellent agreement with reported values, −0.81(−0.64) at more expensive computation B3LYP/6-31G* [23].

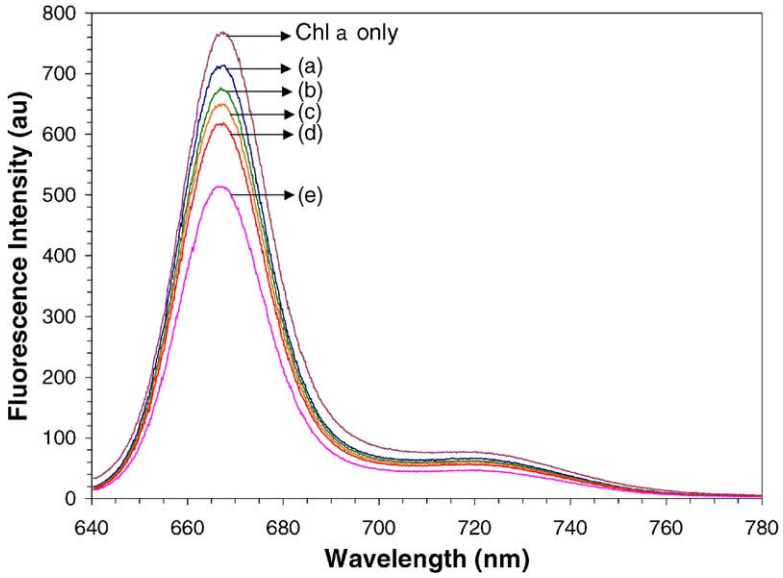

Fig. 6. Effect of addition of ITNF on the emission spectrum of chl a in dichloromethane: where [ITNF] is (a) 2.18×10^{-4} M, (b) 3.26×10^{-4} M, (c) 4.35×10^{-4} M, (d) 5.44×10^{-5} M, and (e) 1.09×10^{-3} M.

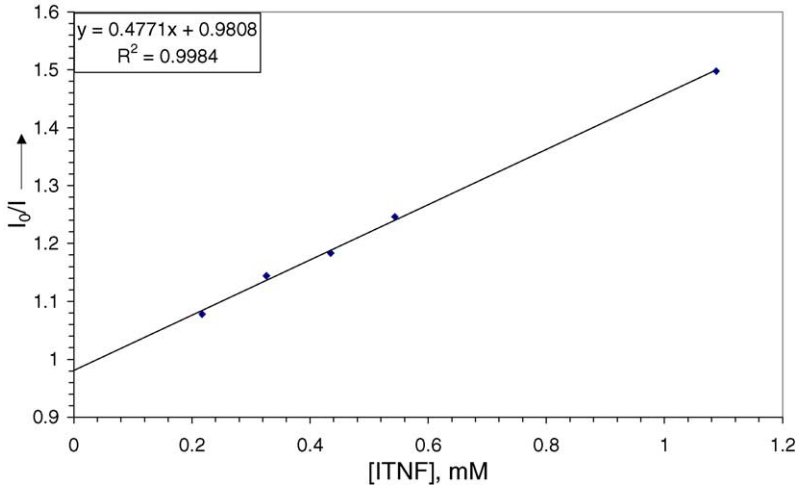

Fig. 7. Linear Stern Volmer plot for chl a with increasing concentrations of ITNF (0–1 mM) in dichloromethane.

Table 5 summarizes measured and calculated ground state parameters. These results support the fact that the binding energies increase as a function of both electron affinity and dipole moment of the quencher. Molecular mechanics predictions of the van der Waals energies between chl a and the acceptor molecules follow the same general trend as the measured free energy values. What is interesting is that the computed geometries of the complexes (for example see Fig. 8) are in accord with the proposed binding site in the previous work [7]. The computed enthalpy and electron affinity values follow the same trend as experimental parameters [17]. However, the discrepancies in the numbers are due to systems in different phases. That is, all computed values are for systems in the gas phase whereas the experimental parameters are in the liquid phase. Solvation effects play a significant role in the complexation of chlorophyll a to the investigated acceptor molecules. In general, the predicted binding trends in the gas phase follow the measured binding trends in liquid phase. The experimental dipole moment of fluorene (0.83 D) compares favorably with the computed number of 0.52 D. No experimental dipole moments were obtained for the investigated trinitro fluorene derivatives. However, the measured dipole moments for fluorenone and 2-nitrofluorenone are 3.35 and 6.04 D, respectively [24]. Computation of 3.07 and 6.56 D for fluorenone and 2-nitrofluorenone, respectively, tested the reliability of the calculated dipole moments with the B3LYP functional and 3-21 basis set. These calculations provide support for the dipole moment trends computed for the trinitro derivatives.

The average measured distance between Mg in chlorophyll a structure and position nine carbon in the fluorene moeity was 4.23 Å, however, this distance was shorter, 3.39 Å, for the chl a/fluorene system as shown in Fig. 9. This distance remained somewhat constant with all the investigated trinitro substituted fluorene derivatives consistent with the recently reported observation of π–π (face to face) stacking interactions between benzene dimers. However, the distance between benzene dimers is much shorter, ∼3.70 Å [25]. The latter is due to differences in the selected basis set. The molecular mechanics calculations are simply used for approximation purposes. It is known that diffusion functions also have a significant effect on the binding energy of weakly bound complexes [26].

Table 5
Summary of results – ground state parameters

Parameters	Interactions of chl a with acceptor [A]						
Binding energy in CH_2Cl_2 (experiment), K_a (kcal/mol)	Fluorene 1.78	TNF 2.65	TNFO 2.75	TFPR 3.61	TNFM 4.56	TFPH 4.78	
Binding energy in CH_3CN (experiment), K_a (kcal/mol)	Fluorene 2.41	TFPH 3.37	TFPR 4.59	TNFM 4.78			
Calculated electron affinity (Gaussian 03 W) (eV)	Fluorene −0.68	TFPH 2.36	ITNF 2.40	TNF 2.42	TFPR 2.56	TNFO 2.80	TNFM 3.25
Calculated dipole moment (Gaussian 03 W) (D)	Fluorene 0.520	TNFO 0.982	TNFM 2.54	TFPR 2.56	TNF 2.61	ITNF 4.48	TFPH 7.06
Calculated dipole moment (PC Model 7.5 MMX) (D)	Fluorene 0.186	TNFO 0.791	TNFM 2.23	TNF 2.57	TFPH 2.90	ITNF 3.38	TFPR 4.07
van der Waals interaction (PC Model 7.5) (kcal/mol)	Fluorene −12.8	TFPR 0.470	TNF 0.790	TNFO 1.98	ITNF 2.82	TNFM 4.73	TFPH 6.12

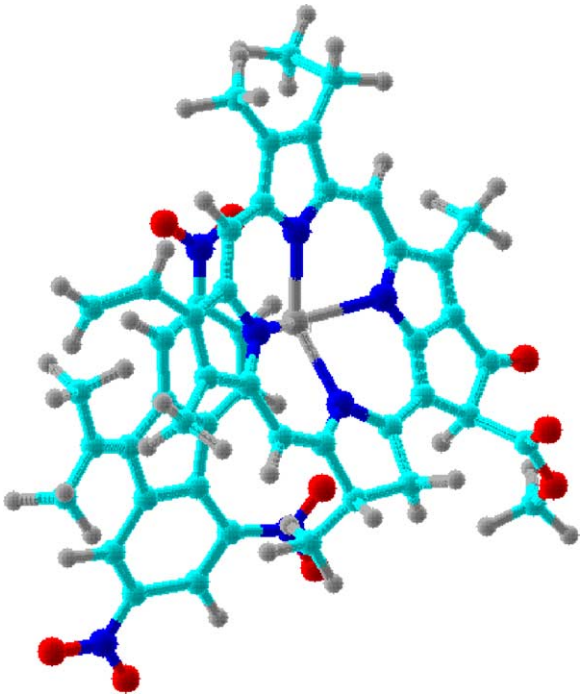

Fig. 8. Predicted structure of chl a/ITNF complex (top view) in the gas phase using PC Model 7.5 software package with MMX force field.

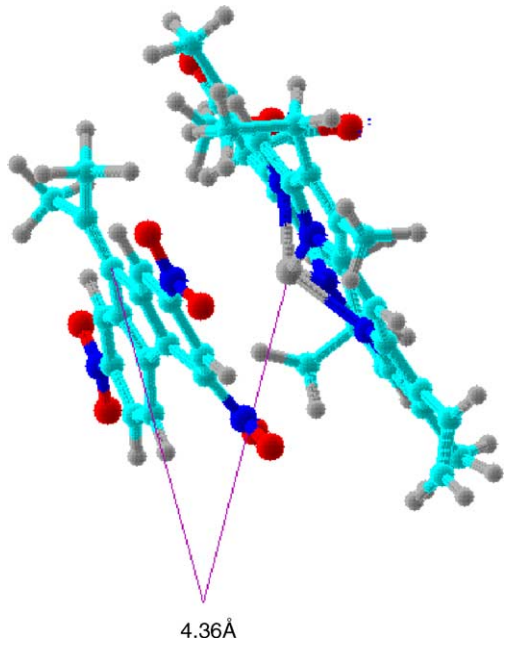

Fig. 9. Predicted structure of chl a/ITNF complex (side view) in the gas phase with the distance between the Mg and 9-carbon atom indicated at 4.36 Å.

4. Conclusion

We have shown in this study that the binding energy of fluorene and trinitro-substituted fluorene derivatives depends on solvent polarity. The investigated chl a/acceptor complexes are stabilized in a more polar solvent, acetonitrile. Theoretical calculations using continuum modeling of solvation will be applied to these systems, to determine the effects of solvent polarity on the binding mechanisms and this work will be published elsewhere. The quenching constants also follow the same trend as the association constants, with the exception of the chl a/fluorene system. The latter is possibly due to the fact that fluorene is a poor electron acceptor. Molecular modeling with Gaussian and PC Model support experimental observations. Moreover, both dipole moment and electron affinity of the quencher or acceptor molecule play a role in the binding of chl a to these molecules. We have also provided theoretical support for the binding site of these quenchers. The predicted binding location on the chlorophyll molecule is in agreement with the suggested position of these types of molecules from previously reported NMR data.

Acknowledgements

Financial support from Kentucky National Science Foundation Experimental Program to Stimulate Competitive Research (KY NSF EPSCoR) through REG grant (537111) is gratefully acknowledged.

References

[1] L.V. Natarjan, J.E. Ricker, R.E. Blankenship, R. Chang, Photochem. Photobiol. 39 (1984) 301.
[2] K.K. Karukstis, S.M. Gruber, J.A. Fruetel, S.C. Boegeman, Biochim. Biophys Acta 932 (1988) 84.
[3] N.G. Bukhov, G. Sridharan, E.A. Egorova, R. Carpentier, Biochim. Biophys Acta 1604 (2003) 115.
[4] L.V. Natarjan, R.E. Blankenship, Photochem. Photobiol. 38 (1983) 329.
[5] M. Iwaki, S. Kumazaki, K. Yoshihara, T. Erabi, S. Itoh, J. Phys. Chem. 100 (1996) 10802.
[6] L.V. Natarjan, M.T. Buthelezi, L.R. Lim, R. Chang, Chem. Phys. Lett. 197 (1992) 145.
[7] P.R. Droupadi, V. Krishnan, J. Phys. Chem. 89 (1985) 909.
[8] G.S. Beddard, S. Carlin, L. Harris, G. Porter, C.J. Tredwell, Photochem. Photobiol. Part A Chem. (1977) 433.
[9] J.R. Larry, Q. Van Winkle, J. Phys. Chem. 73 (1969) 570.
[10] N. Kraub, Curr. Opinion Chem. Biol. 7 (2003) 540.
[11] P. Jordan, P. Fomme, H.T. Witt, W. Saenger, N. Kraub, Nature 411 (2001) 909.
[12] N. Kamiya, J.R. Shen, Proc. Natl. Acad. Sci. U.S.A. 100 (2003) 98.
[13] A.B. Parusel, S. Grimme, J. Phys. Chem. B 104 (2000) 5395.
[14] D. Sundholm, Chem. Phys. Lett. 317 (2000) 545.
[15] PCModel V7.5, Molecular Modeling Software, Serena Software, Bloomington, IN.
[16] M.J. Frisch, G.W. Trucks, H.B. Schlegel, G.E. Scuseria, M.A. Robb, J.R. Cheeseman, J.A. Montgomery Jr., T. Vreven, K.N. Kudin, J.C. Burant, J.M. Millam, S.S. Iyengar, J. Tomasi, V. Barone, B. Mennucci, M. Cossi, G. Scalmani, N. Rega, G.A. Petersson, H. Nakatsuji, M. Hada, M. Ehara, K. Toyota, R. Fukuda, J. Hasegawa, M. Ishida, T. Nakajima, Y. Honda, O. Kitao, H. Nakai, M. Klene, X. Li, J.E. Knox, H.P. Hratchian, J.B. Cross, C. Adamo, J. Jaramillo, R. Gomperts, R.E. Stratmann, O. Yazyev, A.J. Austin, R. Cammi, C. Pomelli, J.W. Ochterski, P.Y. Ayala, K. Morokuma, G.A. Voth, P. Salvador, J.J. Dannenberg, V.G. Zakrzewski, S. Dapprich, A.D.

Daniels, M.C. Strain, O. Farkas, D.K. Malick, A.D. Rabuck, K. Raghavachari, J.B. Foresman, J.V. Ortiz, Q. Cui, A.G. Baboul, S. Clifford, J. Cioslowski, B.B. Stefanov, G. Liu, A. Liashenko, P. Piskorz, I. Komaromi, R.L. Martin, D.J. Fox, T. Keith, M.A. Al-Laham, C.Y. Peng, A. Nanayakkara, M. Challacombe, P.M.W. Gill, B. Johnson, W. Chen, M.W. Wong, C. Gonzalez, J.A. Pople, Gaussian 03, Revision B.05, Gaussian, Inc., Pittsburgh, PA, 2003.
[17] P.R. Droupadi, V. Krishman, Biochim. Biophys Acta 894 (1987) 284.
[18] F.C. Pennington, H.H. Strain, W.A. Svec, J.J. Katz, J. Am. Chem. Soc. 86 (1964) 1418.
[19] C.P. Nash, J. Phys. Chem. 64 (1960) 950.
[20] J.B. Foresman, A. Frisch, Exploring Chemistry with Electronic Structure Methods, 2nd ed., Gaussian, Inc., 1995/1996.
[21] T.K. Mucherjee, Tetrahedron 24 (1968) 721.
[22] V. Kampars, O. Neilands, Russ. Chem. Rev. 40 (1977) 503.
[23] J.M. Gonzales, C.J. Barden, S.T. Brown, P. von, R. Schleyer, H.F. Schaefer III, Q. Li, J. Am. Chem. Soc. 125 (2003) 1064.
[24] E.D. Hughes, C.G. Le Fevre, R.J.W. Le Fevre, J. Am. Chem. Soc. (1937) 202.
[25] M.O. Sinnokrot, C.D. Sherrill, J. Phys. Chem. A 107 (2003) 8377.
[26] M.O. Sinnokrot, E.F. Valeev, C.D. Sherrill, J. Am. Chem. Soc. 124 (2003) 10887.